Research Article

Molecular Cancer Therapeutics

ErbB-Inhibitory Protein: A Modified Ectodomain of Epidermal Growth Factor Receptor Synergizes with Dasatinib to Inhibit Growth of Breast Cancer Cells

Jyoti Nautiyal[1,2,3], Yingjie Yu[1,4], Amro Aboukameel[2,4], Shailender S. Kanwar[1,4], Jayanta K. Das[1,4], Jianhua Du[1,4], Bhaumik B. Patel[1,2,4], Fazlul H. Sarkar[2,5], Arun K. Rishi[1,2,3,4], Ramzi M. Mohammad[2,4], and Adhip P.N. Majumdar[1,2,3,4]

Abstract

Many solid tumors, including breast cancer, show increased activation of several growth factor receptors, specifically epidermal growth factor receptor (EGFR) and its family members as well as c-Src, a nonreceptor tyrosine kinase that promotes proliferation, inhibits apoptosis, and induces metastasis. We hypothesize that inhibition of c-Src and EGFRs will be an effective therapeutic strategy for triple-negative breast cancer. To test our hypothesis, we used a c-Src–specific inhibitor dasatinib (BMS-354825; Bristol-Myers Squibb) and our newly developed ErbB-inhibitory protein (EBIP), a potential pan-ErbB inhibitor, in breast cancer cells. EBIP is composed of 1 to 448 amino acids of the ectodomain of human EGFR to which the 30–amino acid epitope (known as "U" region) of rat EGFR-related protein is fused at the COOH-terminal end. The combination of dasatinib and EBIP was found to be highly effective in inhibiting the growth of four different breast cancer cells (MDA-MB-468, SKBr-3, MDA-MB-453, and MDA-MB-231) that express different levels of EGFRs. In EGFR-overexpressing MDA-MB-468 cells, the combination, but not monotherapy, markedly stimulated apoptosis mediated by caspase-9 and caspase-8 and attenuated activation of EGFR and Src as well as tyrosine kinase activity. EBIP also inhibited heregulin-induced activation of HER-2 and HER-3 in MDA-MB-453 breast cancer cells. The combination therapy was highly effective in suppressing tumor growth (~90% inhibition) in MDA-MB-468–derived xenografts in severe combined immunodeficient mice. The latter could be attributed to induction of apoptosis. We conclude that combining dasatinib and EBIP could be an effective therapeutic strategy for breast cancer by targeting EGFRs and Src signaling. *Mol Cancer Ther; 9(6); 1503–14. ©2010 AACR.*

Introduction

Breast cancer is the second leading cause of cancer-related deaths among females, next only to lung cancer (1). It is a complex disease. Based on transcriptional profiling, breast cancer is currently identified in five distinct subtypes: luminal A and B, normal breast like, HER-2 overexpressing, and basal like (2, 3). Basal-like breast cancer, which shows the absence of hormone receptors (estrogen receptor and progesterone receptor) without amplification of HER-2, is referred to as triple-negative breast cancer. As a group, basal-like cancers comprise ~80% of triple-negative cancers (3). At present, there is controversy about the classification of basal and triple-negative breast cancers. For the sake of simplicity, these two terms are frequently used interchangeably. Triple-negative breast cancer is found to be more common among African-American and BRCA1 mutation carriers (4). It is associated with aggressive histology, poor prognosis, and unresponsiveness to usual endocrine therapies (2, 5–7), highlighting the need for new therapeutics/strategies.

Several targeted therapies for epidermal growth factor receptor (EGFR) and its family members have been developed for treatment of many malignancies, including breast cancers (8, 9). Although trastuzumab, monoclonal antibodies to HER-2, is being used for treatment of HER-2–overexpressing breast cancer, it is not an effective therapy for triple-negative breast cancer (9). The fact that the extracellular or ectodomain of EGFR is essential for ligand binding and subsequent homodimerization/heterodimerization of the receptor raises the possibility that this domain of EGFR could be used to inhibit EGFR functions and could, therefore, be developed into an anticancer

Authors' Affiliations: [1]Veterans Affairs Medical Center, [2]Karmanos Cancer Institute, [3]Graduate Program in Cancer Biology, School of Medicine, and Departments of [4]Internal Medicine and [5]Pathology, Wayne State University, Detroit, Michigan

Note: Supplementary material for this article is available at Molecular Cancer Therapeutics Online (http://mct.aacrjournals.org/).

J. Nautiyal and Y. Yu contributed equally to this work.

Corresponding Author: Adhip P.N. Majumdar, John D. Dingell Veterans Affairs Medical Center, 4646 John R, Room B-4238, Detroit, MI 48201. Phone: 313-576-4460; Fax: 313-576-1112. E-mail: a.majumdar@wayne.edu

doi: 10.1158/1535-7163.MCT-10-0019

agent. Indeed, EGFR-related protein (ERRP), a 53- to 55-kDa protein, which we isolated from the rat gastroduodenal mucosa, targets multiple members of the EGFR family and inhibits growth of several epithelial cancers, including the gastric mucosa, colon, and pancreas (10–16). ERRP is composed of three of the four extracellular subdomains of EGFR and a 30–amino acid unique epitope (termed "U") at the COOH terminus (10, 14). Although the 30–amino acid U region of ERRP possesses no homology with any known protein, antibodies raised against this epitope strongly cross-react with proteins in the liver, pancreas, gastric mucosa, and colon of humans (8, 10, 11). This suggests that the U region harbors an antigenic epitope that is present in humans. The fact that ERRP was isolated from the rat that showed ~85% homology to the ectodomain of human EGFR (hEGFR) raised the possibility of inducing antigenic response in humans. This had prompted us to generate an expression plasmid of truncated hEGFR ectodomain containing the U region of ERRP, which we referred to as ErbB-inhibitory protein (EBIP). In the present investigation, we studied the growth-inhibitory properties of EBIP in breast cancer cells that express varying levels of EGFR and its family members.

Furthermore, the fact that c-Src may also be involved in the development and progression of breast cancer led us to study the effectiveness of the c-Src inhibitor dasatinib (BMS-354825), alone or together with EBIP, in inhibiting growth of breast cancer cells. Dasatinib (BMS-354825) was identified as a highly potent, ATP-competitive inhibitor of Src family kinases and Abl kinases (17), which is approved for imatinib-resistant chronic myelogenous leukemia and (Philadelphia chromosome–positive) acute lymphoblastic leukemia treatment (18). Dasatinib has been shown to exhibit antiproliferative activity in both hematologic and solid tumors and is currently in clinical trial for triple-negative breast cancer. Dasatinib has also been shown to inhibit processes of metastasis such as migration and invasion (18–25).

Materials and Methods

Cell lines and cell culture

Human breast cancers MDA-MB-468, SKBr-3, MDA-MB-453, and MDA-MB-231 cells, obtained from the American Type Culture Collection, were used to investigate the mechanisms of growth inhibition by dasatinib and/or EBIP. All cell lines were maintained in DMEM, as described previously (26).

Chemicals

DMEM, fetal bovine serum, and antibiotic/antimycotic were obtained from Life Technologies. Dasatinib was obtained partially from Bristol-Myers Squibb through Material Transfer Agreement and purchased from LC Laboratories. Protease inhibitor cocktail, MTT, and other chemicals were obtained from Sigma. Acridine orange and ethidium bromide were purchased from BD Biosciences. Acridine orange/ethidium bromide mixture was prepared according to the manufacturer's instruction. Anti–phospho-EGFR (Tyr^{845}), phospho-EGFR (Tyr^{1173}), phospho–HER-2 (Tyr^{877}), phospho–HER-3 (Tyr^{1289}), phospho-Akt (Ser^{473}), phospho–extracellular signal-regulated kinase p44/42, c-Src, and phospho-Src (Tyr^{416}) were purchased from Cell Signaling. Antibodies to β-actin were purchased from Chemicon International, Inc. Recombinant transforming growth factor-α (TGF-α) and heregulin were procured from Calbiochem. Antibodies to α-tubulin were purchased from Oncogene. Antibodies to poly(ADP-ribose) polymerase (PARP) and EGFR were obtained from Santa Cruz Biotechnology, Inc., and anti-V5 was purchased from Invitrogen. *In Situ* Cell Death Detection Kit, POD was obtained from Roche Diagnostics GmbH to do terminal deoxynucleotidyl transferase–mediated dUTP nick end labeling (TUNEL) assay.

Generation of EBIP expression constructs

The following expression constructs were generated.

Rat EGFR ectodomain (ERRP without U region; referred to as ERRP-447). Rat EGFR sequences corresponding to ERRP (amino acids 1–447) were PCR amplified using the following primers: 5′-ATGCGACCCTCAGGGACCGCGAG-3′ (forward) and 5′-CCGCTCGAGGATGTTATGTTCAGGCCGAC-3′ (reverse). The PCR product was cut with *Xho*I restriction enzymes and subcloned into *Eco*RV + *Xho*I cut pMT/His-V5B vector (Invitrogen) to obtain a recombinant plasmid for expression of V5-His–tagged rat EGFR ectodomain sequences.

hEGFR ectodomain (referred to as hEGFR-501). hEGFR sequences from amino acids 1 to 501 were PCR amplified using the following primers: 5′-CGCAAGCTTCGGGAGAGCCGGAGCGAGC-3′ (forward) and 5′-CCGCTCGAGGCCTTGCAGCTGTTTTCAC-3′ (reverse). The reason for selecting position 501 for truncation was that this truncated ectodomain of hEGFR was shown by Elleman et al. (27) to bind EGFR ligands (e.g., EGF and TGF-α) with 13- to 14-fold higher affinity than the full-length EGFR ectodomain. The PCR product was cut with *Xho*I restriction enzyme and subcloned into *Eco*RV + *Xho*I cut pMT/His-V5B vector to obtain a plasmid for expression of His-V5–tagged hEGFR-501 ectodomain sequences.

hEGFR ectodomain fused with U region (referred to as hEGFR-448+U or EBIP). EBIP was synthesized by fusing the U region from ERRP to hEGFR ectodomain (referred to as hEGFR-448+U or EBIP). The following steps were taken to construct the expression vector.

Step i. hEGFR sequences from amino acids 1 to 448 were first PCR amplified using the following primers: 5′-CGCAAGCTTCGGGAGAGCCGGAGCGAGC-3′ (forward) and 5′-CGCGTTAACGATGTTATGTTCAGGCT-3′ (reverse). This PCR product was digested with *Hin*dIII and *Hpa*I and gel purified for subsequent three-way ligation.

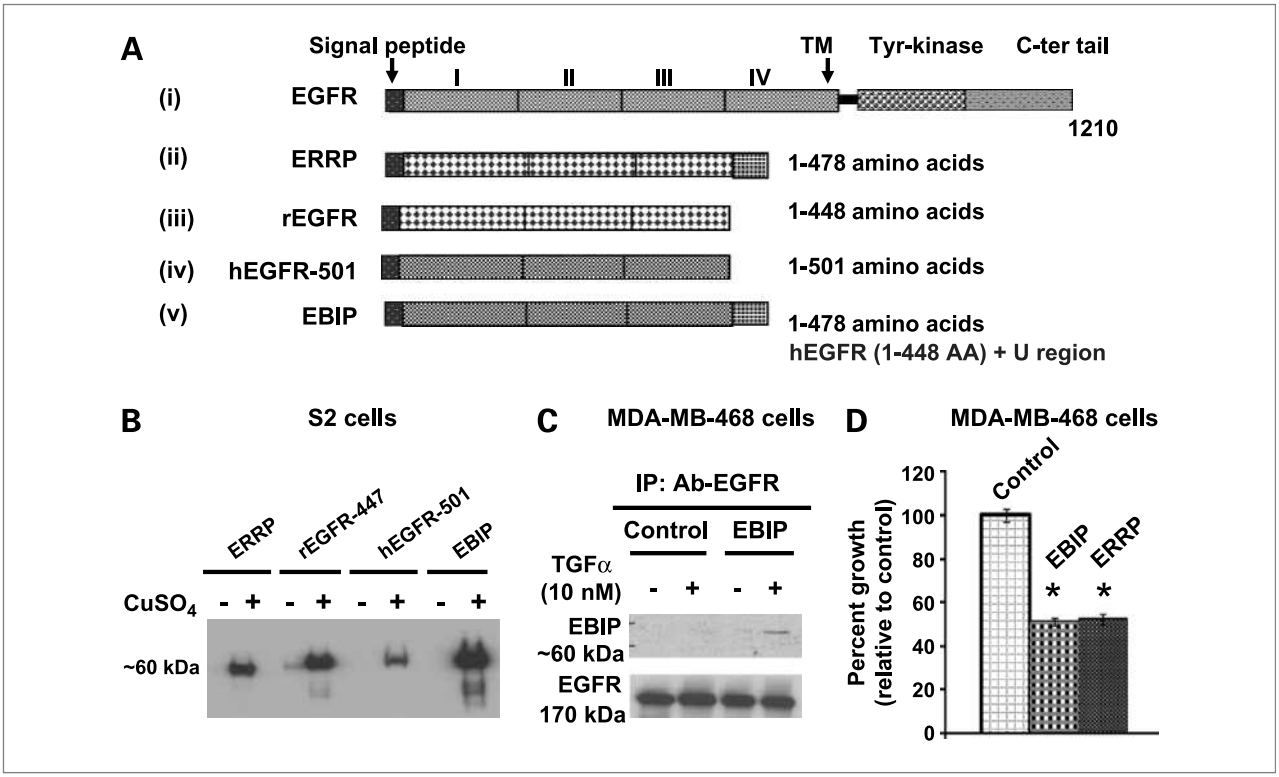

Figure 1. A, schematic representation of full-length hEGFR (i) and four different plasmid constructs of (ii) rat ERRP (amino acids 1–478), (iii) rat EGFR ectodomain (ERRP without U region; referred to as ERRP-448), (iv) Human hEGFR ectodomain (referred to as hEGFR-501), and (v) hEGFR ectodomain fused with U region (referred to as hEGFR-448+U or EBIP). B, synthesis of recombinant proteins by *Drosophila S2* cells in the absence (–) or presence (+) of $CuSO_4$ as determined by Western blot analysis of the cell lysates. Recombinant proteins containing both His and V5 tags were purified using His tag and immunoblotted with V5 antibody. C, Western blot analysis of EBIP localization in response to TGF-α induction of breast cancer cells. After 8 h of incubation with EBIP, MDA-MB-468 cells, which were serum starved, were induced with TGF-α. The cell lysates were immunoprecipitated with EGFR antibodies overnight and the immunoprecipitates were subsequently subjected to Western blot analysis with V5 antibody for EBIP detection. D, inhibition of growth of MDA-MB-468 cells in response to immunoaffinity-purified EBIP and ERRP.

Step ii. The U region epitope from ERRP was synthesized as oligonucleotides with codons optimized for human expression. The following oligonucleotides were used: oligo 1, 5′-AGCGCGGCGCCGTGGCAGGTTCCGTCTCTTTCTTGGCAGGCCGTTACCAGGCCG-3′; oligo 2, 5′-CTGGTAACGGCCTGCCAAGAAAGAGACGGAACCTGCCACGGCGCCGCG-3′; oligo 3, 5′-CTTCATCCGCTAGCCCAAAACCGCGTCAGCCTGGGACACAGGCCCCTCTAGACGC-3′; and oligo 4, 5′-CCGCGTCTAGAGGGGCCTGTGTCCCAGCTGACGCGGTTTTGGGCTAGCGGATGAAGCGGC-3′.

The oligonucleotides were phosphorylated at the respective 5′ ends using T4 polynucleotide kinase and annealed as follows: oligos 1 + 2 and oligos 3 + 4. The annealed products were ligated to obtain a contiguous U region sequence. This double-stranded U region sequence was then used as template in a PCR using the following primers: 5′-AGCGCGGCGCCGTGGCAG-3′ (forward) and 5′-CCGCGTCTAGAGGGGCCT-3′ (reverse). The PCR product was cut with a combination of *Sfo*I and *Xba*I restriction enzymes, and the product was gel purified.

Step iii. The PCR-amplified products from steps i and ii were ligated into *Hin*dIII plus *Xba*I cut vector plasmid pcDNA-3/myc-His-A to obtain a recombinant plasmid for expression of myc-His–tagged hEGFR+U protein.

Step iv. The cDNA insert of the recombinant plasmid from step iii above was PCR amplified using the forward primer from step i and the reverse primer from step ii. The PCR product was then cut with *Xba*I and ligated into *Eco*RV plus *Xba*I cut pMT/V5-HisA vector (Invitrogen) to obtain a construct for expression of V5/His-tagged hEGFR+U protein. The V5 and 6×His tags are located at the COOH-terminal end of the plasmid (just after the U region).

Rat ERRP. Rat ERRP has been described previously and detailed in the U.S. Patent 6,399,743 and 6,582,934 (GenBank accession number AF187818). It is composed of 478 amino acids.

All the constructs were sequenced to confirm the validity of the inserts.

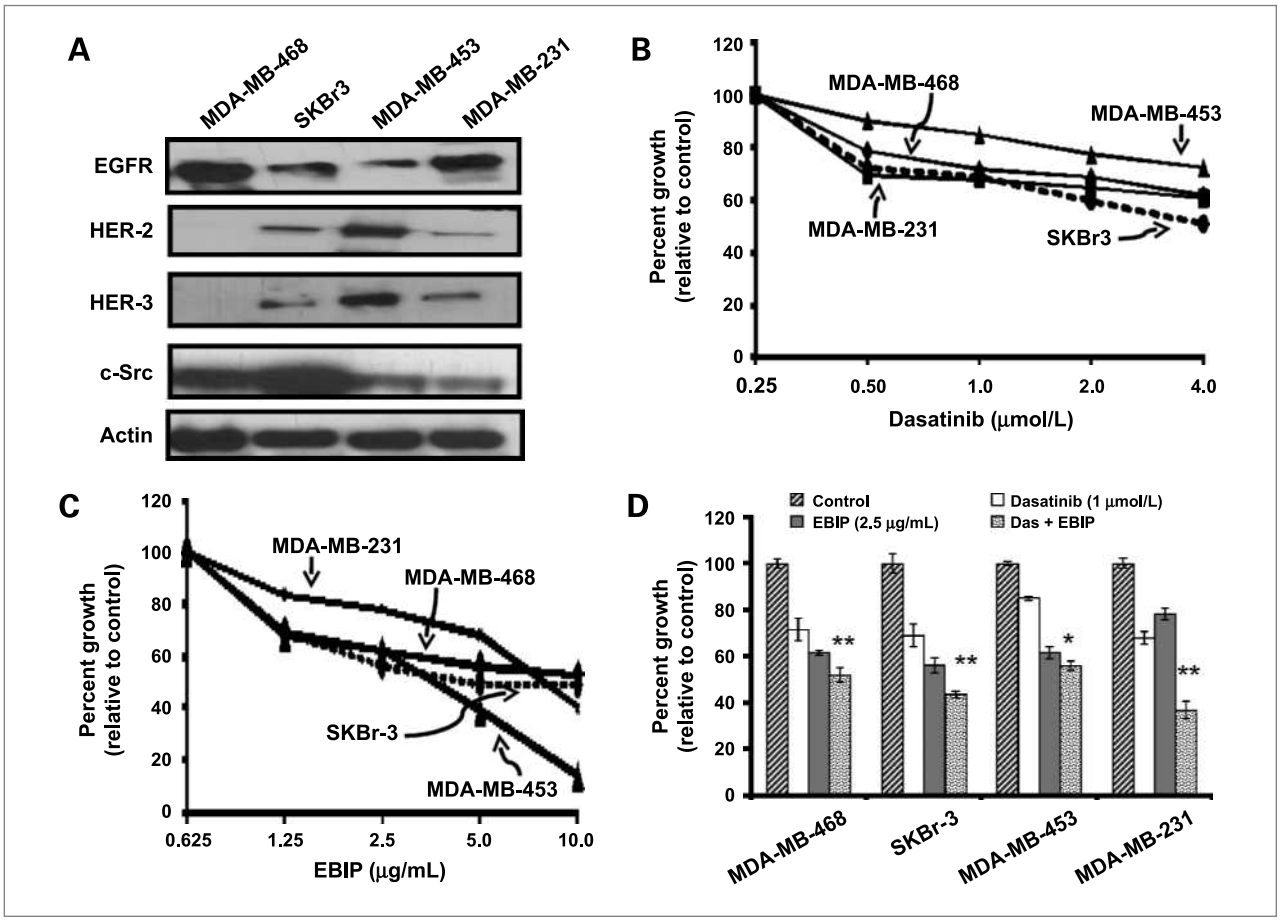

Figure 2. A, Western blot showing the levels of EGFR, HER-2, and HER-3 in four different human breast cancer cells. Effects of EBIP and/or dasatinib on growth of human breast cancer cells expressing varying levels of EGFR members. Growth was determined by MTT assay after 48 h of exposure to increasing doses of dasatinib (B) and EBIP (C). D, combined therapy of dasatinib (Das; 1.0 μmol/L) and EBIP (2.5 μg/mL purified protein) in human breast cancers. *, $P < 0.05$, compared with individual drugs. Columns, mean of six observations; bars, SD.

Generation of recombinant EBIP

Recombinant EBIP was generated using the *Drosophila* expression system as described earlier for ERRP by Marciniak et al. (11). In brief, expression vector pMT/V5-HisA containing the entire reading frame of ERRP, rEGFR-448, hEGFR-501, or EBIP cDNA was transfected into *Drosophila S2* cells with pCoHygro plasmid (Invitrogen), which confers hygromycin resistance. The stable cell line was induced with 0.5 mmol/L $CuSO_4$ to express respective fusion protein. Proteins were purified from the crude cell lysate using polyhistidine antibodies (Invitrogen) conjugated to Sepharose 4B (Pharmacia) as described by Marciniak et al. (11). The activity of ERRP/EBIP was determined by MTT assay as reported earlier (11). ERRP/EBIP with at least 80% growth-inhibitory effect was selected for all experiments.

Growth inhibition assay

Cell growth was determined by MTT assay (26). Briefly, 5,000 cells per well were treated in 96-well culture plates for 24 or 48 hours in the absence (control) or presence of affinity-purified EBIP and/or dasatinib, as described in the figure legends, with six replicates. At the end of the treatment period, cells were incubated with 10% of 5 mg/mL stock of MTT and incubated for 3 hours at 37°C as described previously (26).

Analysis of interaction between two drugs

Combination index (CI) method adapted for *in vitro* anticancer drug testing was used to determine the nature of interaction between the two agents as described previously (28). Based on CI values, the extent of synergism/antagonism may be determined. In general, CI < 1 suggests synergy, whereas CI > 1 indicates antagonism between the drugs. CI values in the range of 0.9 to 1.10 suggest mainly additive effects of the drugs, those between 0.9 and 0.85 would suggest slight synergy, and values in the range of 0.7 to 0.3 are indicative of moderate synergy. Any value <0.3 will suggest strong synergistic interactions between the drugs.

Western blot analysis

Western blot analysis was done as described previously (26). Briefly, aliquots of cell lysates containing 80 μg protein were separated by SDS-PAGE. Electrophoresed proteins were transferred onto nitrocellulose membranes and detected using specific primary and secondary antibodies. The protein bands were visualized by enhanced chemiluminescence detection kit (Amersham Biosciences/Amersham Pharmacia Biotech). The membranes were reprobed for β-actin as loading control. All Western blots were done at least thrice for each experiment.

Assessment of apoptosis

DNA histone fragmentation ELISA. Approximately 1×10^5 cells per well were plated and treated the same way as described above. After 24 hours, the cells were lysed, and apoptosis was determined using the Cell Death Detection ELISA^{PLUS} kit from Roche Diagnostics.

Acridine orange staining. The cells were treated and collected as described for DNA fragmentation assay. They were washed once with cold 1× PBS and resuspended in 1× PBS (0.5×10^6 to 1×10^6 cells/mL). Cell suspension (50 μL) was stained with 50 μL of acridine orange/ethidium bromide mixture according to the manufacturer's instructions. Within 5 minutes of addition of the acridine orange/ethidium bromide mixture, 10 μL aliquots containing 300 to 500 cells were counted under a fluorescent microscope. Cells that stained positive for acridine orange fluoresced green (live cells), whereas cells that stained positive for ethidium bromide fluoresced red (dead cells). Results were calculated as (ethidium bromide–stained cells/ethidium bromide– or acridine orange–stained cells) × 100.

Tyrosine kinase assay

EGFR kinase activity was determined using the Chemicon Assay kit essentially according to the manufacturer's instructions. Briefly, MDA-MB-468 cells were treated for 24 hours with dasatinib and/or EBIP. At the end of the treatment period, cells were collected and lysed and aliquots of 500 μg protein were subjected to immunoprecipitation with anti-EGFR antibody (Santa Cruz Biotechnology) as described previously (11). After overnight incubation at 4°C, the lysates were centrifuged and the Sepharose beads were washed thrice with lysis buffer. Subsequently, the immunobeads were assayed for kinase activity. The samples were read at 450 nm, and the results were presented as relative to untreated control.

Severe combined immunodeficient mice xenografts of MDA-MB-468 cells

Four-week-old female ICR/severe combined immunodeficient (SCID) mice, obtained from Taconic Laboratory, were s.c. injected with 10×10^6 MDA-MB-468 breast cancer cells (11). When tumor burden reached 1,500 to 2,000 mg, mice were euthanized. The tumors were removed, cut into 20 to 30 mg fragment, and subsequently transplanted (s.c.) bilaterally into similarly conditioned 28 animals (11). Once palpable tumors were formed, animals were randomly divided into four groups: control (vehicle), dasatinib (10 mg/kg, every other day gavage), EBIP (s.c.; 25 μg/mouse, every other day), and dasatinib + EBIP. Treatment was started on day 7 and continued until day 23. Animals and tumor burden were followed for up to 55 days. Tumor measurements were carried out at multiple time points during the experimental period. Mice were weighed and monitored for signs of toxicity. Tumor weights in SCID mice were estimated as tumor weight (mg) = $(A \times B^2)/2$, where A and B are the tumor length and width (in mm), respectively. At the end of the experiments, the mice were sacrificed and the residual tumors were harvested for Western blot analysis and fixed in buffered formalin and processed for immunohistochemistry as described previously (11, 29).

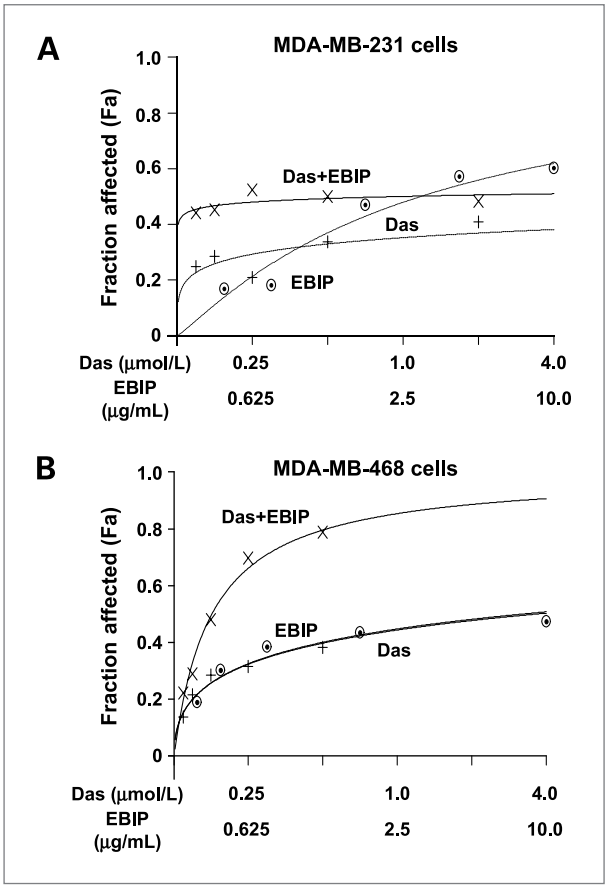

Figure 3. Typical dose-response curves for EBIP and/or dasatinib in MDA-MB-231 (A) and MDA-MB-468 (B) cells produced by fixed-ratio method. Fraction of breast cancer cells affected by different combination of dasatinib and EBIP (fixed ratio) is higher than either agent alone. Fa represents the fraction of cells that is growth inhibited in response to dasatinib and/or EBIP. This is calculated as 1 – fraction of surviving cells. Fa values for each treatment were used to conduct synergy analysis by CalcuSyn software as described in Materials and Methods.

Table 1. Combination indices for dasatinib and EBIP combination therapy, as computed by Calcusyn for MDA-MB-231

Dasatinib (μmol/L)	Fa	EBIP (μg/mL)	Fa	Dasatinib + EBIP (Fa)	CI
0.50	0.354	1.25	0.105	0.462	0.076
1.0	0.322	2.5	0.223	0.506	0.128
2.0	0.353	5.0	0.387	0.151	0.247
4.0	0.392	10.0	0.535	0.544	0.447

NOTE: CI < 1.0 suggests synergy.
Abbreviations: Fa, fraction affected; CI, confidence interval.

Immunohistochemical analysis

For immunohistochemical staining, an immunoperoxidase method was used with a streptavidin-biotinylated horseradish peroxidase complex (Dako) as described previously (11, 29). Briefly, sections of formalin-fixed, paraffin-embedded tissue blocks were deparaffinized and rehydrated in 0.1 mol/L PBS (pH 7.4), treated for 15 minutes with blocking serum (Vector Laboratories), and subsequently incubated overnight in a refrigerated humidity chamber with antibodies to either anti-V5 or phospho-EGFR (Tyr^{1173}). The next day, the slides were washed thrice in 1×-PBS and incubated with a biotin-conjugated secondary antibody at room temperature for 30 minutes and finally with peroxidase-conjugated streptavidin at room temperature for 30 minutes. Peroxidase activity was detected with the enzyme substrate 3-amino-9-ethylcarbazole. For negative controls, sections were treated in the same way except that they were incubated with 1×-TBS instead of the primary antibody. All slides were coverslipped and examined under 10× objective.

Determination of apoptosis by TUNEL assay

Paraffin-embedded tissues were sectioned as described above, and the TUNEL assay was done to detect apoptotic cells using the *In Situ* Cell Death Detection kit (Roche Applied Science) according to the manufacturer's instructions as described previously (11, 16). 3-Amino-9-ethylcarbazole was used as chromogen, and the sections were counterstained with hematoxylin. Apoptotic cell nuclei appeared as red-stained structures against a blue-violet background. The apoptotic cells within each section were counted with a 10× objective.

Statistical analysis

Unless otherwise stated, data were expressed as mean ± SD. Where applicable, the results were compared by using the unpaired, two-tailed Student's *t* test, as implemented by Excel 2000 (Microsoft Corp.). *P* values of <0.05 were considered statistically significant. One-way ANOVA, SPSS 10.0, was applied for analysis of *in vivo* data.

Results

Generation and characterization of EBIP

Figure 1A depicts a schematic representation of four different plasmid constructs that we generated. They are (ii) full-length rat ERRP (composed of 478 amino acids plus the U region) that we generated earlier, (iii) rat ERRP (composed of 1–448 amino acids) that lacked the U region (referred to as rEGFR-448; ref. 14), (iv) hEGFR ectodomain that contained 1 to 501 amino acids (referred to as hEGFR-501), and (v) hEGFR ectodomain that contained 1 to 448 amino acids plus the U region (hEGFR-448+U; also referred to as EBIP). A schematic representation of hEGFR is also depicted in Fig. 1A, i.

Western blot analysis of *Drosophila S2* cells lysates using antihistidine antibodies revealed a marked stimulation in synthesis of the respective recombinant

Table 2. Combination indices for dasatinib and EBIP combination therapy, as computed by Calcusyn for MDA-MB-468

Dasatinib (μmol/L)	Fa	EBIP (μg/mL)	Fa	Dasatinib + EBIP (Fa)	CI
0.50	0.216	1.25	0.302	0.289	0.714
1.0	0.286	2.5	0.385	0.480	0.249
2.0	0.315	5.0	0.435	0.698	0.070
4.0	0.382	10.0	0.475	0.789	0.051

NOTE: CI < 1.0 suggests synergy.

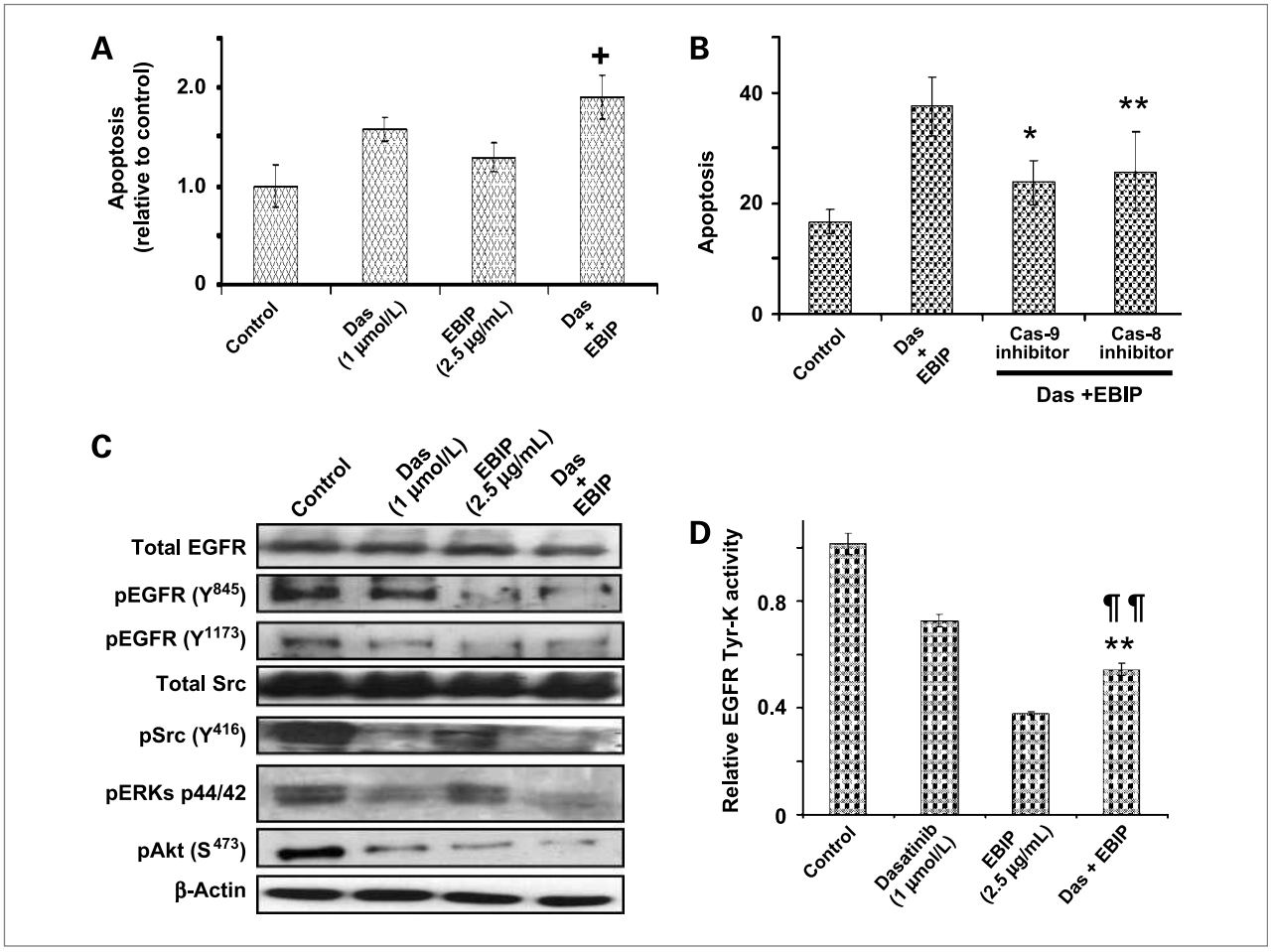

Figure 4. A, effects of EBIP and/or dasatinib on different aspects of growth of MDA-MB-468 breast cancer cells on induction of apoptosis as determined by DNA fragmentation ELISA assay in response to EBIP and/or dasatinib. †, $P < 0.05$, compared with control. B, induction of early apoptosis as determined by acridine orange staining method. Cells were coincubated with combination of dasatinib (1 μmol/L) and EBIP (2.5 μg/mL) and specific inhibitors of caspase-8 or caspase-9. *, $P < 0.05$, compared with combination therapy without caspase inhibitors. C, EGFR signaling and the levels of tyrosine-phosphorylated forms of EGFR and c-Src and their downstream signaling molecules in response to EBIP and/or dasatinib, as determined by Western blot analysis. The experiment was repeated at least thrice. D, tyrosine kinase activity of EGFR. Lysates from cells treated with respective drugs were immunoprecipitated with EGFR. Protein-Sepharose bead complexes were assayed for kinase activity using ELISA-based assay. *, $P < 0.05$, compared with EBIP; ¶, $P < 0.05$, compared with dasatinib alone. Columns, mean of four observations; bars, SD. Data in A and C for control and dasatinib are similar to those recently published by our laboratory (26).

protein following incubation with 0.5 mmol/L $CuS0_4$ for 24 hours (Fig. 1B). In the absence of 0.5 mmol/L $CuS0_4$, no expression of EBIP was detected (Fig. 1B). Because EBIP contains the ligand binding ectodomain of hEGFR, we postulated that it will sequester the ligand, leading to heterodimerization with members of the EGFRs. However, such heterodimers, as has been reported for ERRP and EGFR, would likely to be inactive because ERRP is devoid of the cytoplasmic domain (11). Indeed, when MDA-MB-468 cells containing high levels of EGFR were preincubated with EBIP, followed by induction with TGF-α, we found EBIP to coimmunoprecipitate with EGFR, whereas in the absence of TGF-α (control) no EBIP band could be detected (Fig. 1C). Additionally, growth-inhibitory activity of EBIP was compared with ERRP in human breast cancer cells. Both ERRP and EBIP were found to be equally effective in inhibiting the growth of MDA-MB-468 cells (Fig. 1D). We also compared the growth-inhibitory properties of hEGFR-501, hEGFR-448+U, ERRP, and rEGFR-447 (lacked U region) in colon cancer HCT-116 cells (Supplementary Fig. S1). We observed that whereas ERRP or EBIP at a dose of 20 μg/mL caused a marked 70% inhibition of growth of HCT-116 cells, the same dose of hEGFR-501 or rEGFR-447 produced only a small 20% to 25% inhibition in cellular growth when compared with the corresponding controls (Supplementary Fig. S1). The results suggest that the U region is important for the growth-inhibitory properties of ERRP and EBIP.

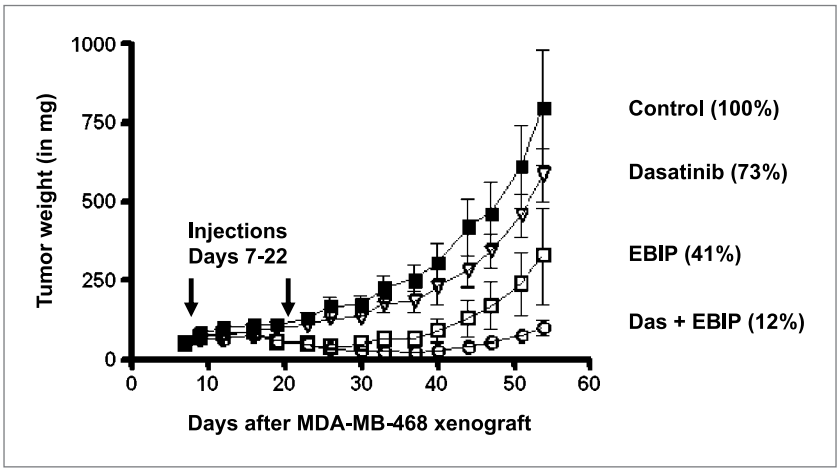

Figure 5. Preclinical efficacy trial of EBIP and/or dasatinib in MDA-MB-468 xenografts of SCID mice. Once palpable tumors developed (day 7), the treatment was initiated with EBIP and/or dasatinib. EBIP (25 μg/animal) was administered s.c. (away from tumor), whereas dasatinib (10 mg/kg) was given orally (gavage), every other day for 16 d. Changes in tumor weight were recorded during the 55-d experimental period. Points, mean; bars, SE.

Earlier, we reported that ERRP is a pan-ErbB inhibitor that targets multiple members of the EGFR family (13). As will be shown below, EBIP also inhibited the growth of different breast cancer cells that express varying levels of EGFR and its family members, indicating potential pan-ErbB nature of this protein. In support of this inference, we observed that whereas both ERRP and EBIP were able to inhibit heregulin-induced activation of HER-2 and HER-3 in MDA-MB-453 breast cancer cells, neither rEGFR-447 nor hEGFR-501 was effective in this matter (Supplementary Fig. S2). Taken together, the results suggest a role for the U region of ERRP in eliciting the growth-inhibitory properties of ERRP and EBIP.

EBIP synergizes with dasatinib to inhibit the growth of human breast cancer cells

In the first set of experiments, we examined the effects of EBIP and dasatinib, each alone or in combination, on the growth of four different breast cancer cells expressing varying levels of EGFRs (Fig. 2A). Both dasatinib and EBIP were effective in inhibiting the growth of all four breast cancer cells (Fig. 2B and C); whereas dasatinib caused a 20% to 40% growth inhibition among different cell lines, EBIP produced a 40% to 90% of the same. When dasatinib (1 μmol/L) and EBIP (2.5 μg/mL) were combined, the magnitude of inhibition of growth was greater than either of the agent alone (Fig. 2D), indicating a greater effectiveness of the combination therapy than monotherapy.

To determine the nature of interactions between EBIP and dasatinib, synergy analysis was done with two triple-negative breast cancer cell lines: MDA-MB-231 and MDA-MB-468. The results of the dose response were analyzed using CalcuSyn software (Biosoft). They show that the combination therapy is superior to monotherapy in both breast cancer cell lines (Fig. 3A and B). The fraction of cells affected in response to each treatment was further used to do synergy analysis with CalcuSyn. The CI, <1.0, which suggests a synergistic interaction between the two agents, was noted for all the combination doses for both breast cancer cell lines (Tables 1 and 2). Taken together, the results suggest that EBIP acts synergistically with dasatinib. In all subsequent experiments, dasatinib at a dose of 1 μmol/L and EBIP at a concentration of 2.5 μg/mL were used in MDA-MB-468 cells. The rationale for using MDA-MB-468 cells is that they express only EGFR, which will result in the formation of homodimers in response to ligand induction.

EBIP and/or dasatinib induce apoptosis and inhibit tyrosine kinase activity

The combined therapy was further tested for its efficacy for induction of apoptosis, which was found to be more effective in MDA-MB-468 cells than either agent alone (Fig. 4A). To further identify the apoptotic pathways, we used specific inhibitors of caspase-8 (Z-IETD-FMK) and caspase-9 (Z-LEHD-FMK). The cells were preincubated with specific inhibitors of caspase-8 or

Table 3. Breast cancer xenograft weight (in mg) among different groups at the end of *in vivo* investigations (day 55)

Study group tumor weight at the end of 55 d	Control (*n* = 5)	Dasatinib (*n* = 5)	EBIP (*n* = 4)	Dasatinib + EBIP (*n* = 6)
Mean ± SD	795 ± 406	584 ± 189	326 ± 304	98.5 ± 59.2
95% CI for mean	546.4–1,043	335.6–832.0	48.77–603.7	128.1–325.1

caspase-9 for 3 hours, subsequently exposed to the combination of EBIP and dasatinib. In the absence of the inhibitors, the combined therapy caused significant apoptosis. However, the addition of specific caspase inhibitor(s) blocked apoptosis induction by the combined therapy, indicating the activation of respective caspase(s) in response to the treatment. This suggests the involvement of both intrinsic (caspase-9) and extrinsic (caspase-8) pathways of apoptosis (Fig. 4B).

EBIP and dasatinib, each alone, inhibited the phosphorylation of EGFR and c-Src, respectively, in MDA-MB-468 cells (Fig. 4C). Again, the combination therapy was much more effective than either agent alone in inhibiting activation of EGFR, c-Src, as well as downstream targets Akt and mitogen-activated protein kinase (Fig. 4C). Dasatinib and/or EBIP inhibited EGFR phosphorylation/activation at both transphosphorylation (Tyr^{845}, mediated by c-Src) and autophosphorylation (Tyr^{1173}) sites. Although dasatinib and EBIP inhibit signaling differentially, the combination therapy, as expected, provided a better therapeutic benefit in achieving a greater inhibition of downstream signaling events (Fig. 4C). Likewise, EGFR tyrosine kinase activity was greatly inhibited by the combined therapy (Fig. 4D). At this time, the slight increase in tyrosine kinase activity in response to the combined therapy is not properly understood. This may be due to the involvement of compensatory mechanisms as reported for signal transducer and activator of transcription 3 (STAT3) in response to dasatinib in head and neck cancer and mesothelioma (22, 30).

Combined therapy is more effective in inhibiting the growth of breast cancer cell–derived xenografts in SCID mice

The objective of this experiment was to examine the effectiveness of monotherapy versus combination therapy on tumor growth. None of the treatments caused any significant change in body weight, indicating no apparent toxicity (data not shown). With respect to tumor growth, dasatinib produced no significant inhibition, whereas EBIP and the combination therapy significantly reduced tumor growth, suggesting effectiveness of the combination therapy ($P < 0.05$; Fig. 5; Table 3). Our results show that whereas dasatinib and EBIP, each alone, caused ~27% and 59% inhibition, combination therapy produced a marked ~90% suppression of tumor growth when compared with the vehicle-treated controls (Fig. 5; Table 3). ANOVA analysis shows that the differences among the groups are significant and the possibility of the results assuming null hypothesis is 0.003 ($P < 0.05$; Table 4). More importantly, our data show that growth of the tumor in the combination treatment group was minimal 32 days after treatment. At this time, the tumor volume was only ~12% of the vehicle-treated control (Fig. 5).

The animals were sacrificed at the end of the 55-day experimental period. To determine whether EBIP reaches the tumor, we analyzed the tissues for the presence of EBIP. Indeed, we saw significant expression of EBIP in the tumors of EBIP-treated mice (Fig. 6A). To determine whether inhibition of tumor growth in SCID mice could be the result of increased apoptosis, we conducted TUNEL assay and examined PARP cleavage in the tumors. As expected, the combined therapy caused a marked induction of apoptosis as evidenced by the increased number of apoptotic cells and PARP (Fig. 6B and C). We also analyzed the tumors for relative abundance of phospho-EGFR by immunohistochemistry using anti–phospho-EGFR (Tyr^{1173}) antibodies. Tumor remnants from mice treated with EBIP or EBIP + dasatinib showed no detectable immunoreactivity for phospho-EGFR, whereas those from the controls and dasatinib-treated mice showed the presence of phospho-EGFR (Supplementary Fig. S3). However, the intensity of phospho-EGFR immunoreactivity in tumors from dasatinib-treated mice was weaker than those from the controls (Supplementary Fig. S3).

Table 4. Results of one-way ANOVA statistical test for the *in vivo* study

Source of variation	Sum of squares	*df*	Mean squares	*F*
Between	1.48E+06	3	4.94E+05	7.22
Error	1.09E+06	16	6.85E+04	
Total	2.58E+06	19		

NOTE: The probability of this result, assuming the null hypothesis, is 0.003.
Abbreviation: *df*, degree of freedom.

Discussion

Interference with activation of EGFR and/or its family members represents a promising strategy for the development of targeted therapies against a wide variety of epithelial cancers because of their preponderance in a variety of neoplastic cells. Indeed, several inhibitors of EGFRs have been developed to interrupt the intracellular signaling induced by activation of EGFR (8, 31, 32). Small-molecule inhibitors of EGFR, gefitinib (Iressa) and erlotinib (Tarceva), approved by the Food and Drug Administration, have now been used for treatment of many epithelial cancers, including breast cancer, but with limited success (8, 31). Although monoclonal antibodies against EGFR (cetuximab) and HER-2 (trastuzumab) showed signs of success in a limited number of patients with tumors that expressed high levels of EGFR or HER-2, failure in others may partly be due to the fact that most solid tumors express more than one member of the EGFR family, and coexpression of multiple EGFR family members leads to an enhanced transforming potential and worsened prognosis (33). Therefore, identification of inhibitor(s), targeting multiple members of the EGFR

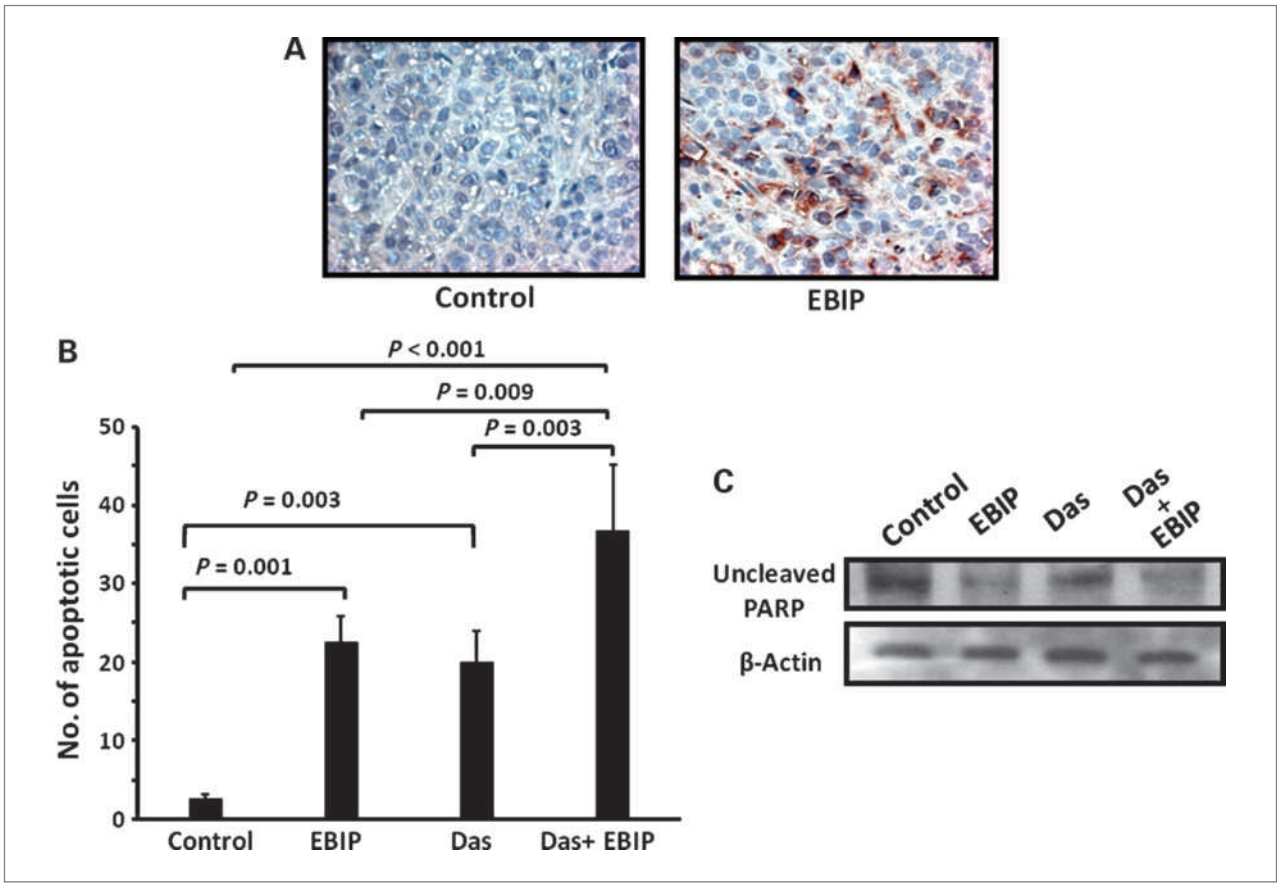

Figure 6. Immunohistochemical demonstration of EBIP in the tumor remnants from mice sacrificed at the end of the experimental period. EBIP was detected in the tumor remnants by V5 antibody staining. A, left, photomicrograph from a vehicle-treated animal; right, photomicrograph from an EBIP-treated animal. B, changes in number of apoptotic cells as determined by TUNEL staining. C, levels of uncleaved PARP as determined by Western blot analysis. Protein extracts were made from the tumor remnants.

family, is likely to provide a therapeutic benefit to a broad range of patient population.

Our current data suggest that EBIP, as has been reported for ERRP (13), is a potential pan-ErbB inhibitor targeting multiple members of the EGFR family. This inference is supported by the observation that EBIP inhibits the growth of several breast cancer cells that express varying levels of different EGFRs. We further show that EBIP forms heterodimer with EGFR in MDA-MB-468 cells, resulting in decreased EGFR signaling. The fact that daily administration of EBIP leads to a significant reduction in the growth of SCID mice xenografts of breast cancer MDA-MB-468 cells, which express very high levels of EGFR and little or no other ErbBs, further corroborates our postulation that EBIP could be used to inhibit growth of EGFR-expressing tumors. This and the fact that EBIP also inhibits growth of several other breast cancer cells that express other members of the EGFR family and also inhibits heregulin-induced activation of HER-2 and HER-3 in breast cancer cells suggest that EBIP, as has been reported for ERRP (8), could potentially be a pan-ErbB inhibitor.

Although the precise mechanisms by which EBIP inhibits activation of EGFR and its family members and in turn cellular growth are not fully understood, earlier studies with ERRP suggest that this peptide, which is structurally and functionally similar to EBIP, inhibits EGFR function by sequestering EGFRs ligand(s), leading to heterodimerization with one of the EGFR family members, which is functionally inactive (12). We believe that the similar phenomenon is responsible for the growth-inhibitory properties of EBIP because EBIP contains the ligand binding domain of EGFR. The possibility that ectodomains of EGFR inhibit EGFR signaling by sequestering their ligands comes from the observation by Garrett et al. (34) that a truncated EGFR with only three of the four extracellular subdomains binds EGF and TGF-α with at least 10-fold higher affinity than the full-length extracellular domain of EGFR, rendering them unavailable for binding to and activation of receptors. Because EBIP, like ERRP, lacks most of the extracellular domain IV, it is reasonable to predict that EBIP will also be effective in preferentially binding/sequestering ligands of EGFR. Our current data support this contention in that

EBIP coimmunoprecipitated with EGFR after induction with TGF-α.

In addition to EGFRs, aberrant activation of c-Src has been observed in many solid tumors, including breast cancers (35–42). Furthermore, co-overexpression of EGFRs and c-Src is associated with higher incidence of metastasis and poor survival (30, 43–47). Because of the involvement of Src in the development and progression of many solid tumors, several Src inhibitors, including dasatinib, have been tested in solid tumors but with limited success (21, 23, 47). This could partly be due to the presence and dominance of compensatory pathways in the cancer cells. For instance, STAT3 pathway is inhibited by dasatinib transiently and through a compensatory pathway (30) and is reactivated as early as 24 hours (22). It has been suggested that STAT3 inhibitors show synergistic interactions with dasatinib in head and neck squamous cell carcinoma (22). Therefore, to achieve a better therapeutic efficacy, targeting multiple pathways simultaneously is warranted. Our observation that dasatinib together with EBIP causes greater inhibition of growth of breast cancer cells *in vitro* and *in vivo* supports our postulation that simultaneous targeting of multiple signaling pathways is an effective therapeutic strategy. We do believe that this is first of a kind study that shows the effectiveness of a combination therapy of EGFR and Src inhibitors in breast cancer.

In conclusion, our data show that (*a*) EBIP is a potential pan-ErbB inhibitor with antitumor activity, (*b*) EBIP synergizes with dasatinib to suppress growth of several breast cancer cells expressing varying levels of EGFRs, and (*c*) the combination therapy is much more effective in inhibiting the growth of breast cancer cell–derived xenografts than monotherapy. We suggest that the combination therapy of EBIP and dasatinib is a potential strategy for the treatment of triple-negative breast cancer.

Disclosure of Potential Conflicts of Interest

No potential conflicts of interest were disclosed.

Grant Support

NIH/National Institute on Aging grant R01 AG014343 (A.P.N. Majumdar), Department of Veterans Affairs (A.P.N. Majumdar and A.K. Rishi), and Susan Komen Foundation (A.K. Rishi).

The costs of publication of this article were defrayed in part by the payment of page charges. This article must therefore be hereby marked *advertisement* in accordance with 18 U.S.C. Section 1734 solely to indicate this fact.

Received 01/13/2010; revised 03/16/2010; accepted 04/02/2010; published OnlineFirst 06/01/2010.

References

1. Jemal A, Siegel R, Ward E, et al. Cancer statistics. CA Cancer J Clin 2008;58:71–96.
2. Sorlie T, Tibshirani R, Parker J, et al. Repeated observation of breast tumor subtypes in independent gene expression data sets. Proc Natl Acad Sci U S A 2003;100:8418–23.
3. Nielsen TO, Hsu FD, Jensen K, et al. Immunohistochemical and clinical characterization of the basal-like subtype of invasive breast carcinoma. Clin Cancer Res 2004;10:5367–74.
4. Foulkes WD, Stefansson IM, Chappuis PO, et al. Germline BRCA1 mutations and a basal epithelial phenotype in breast cancer. J Natl Cancer Inst 2003;95:1482–5.
5. Bauer KR, Brown M, Cress RD, Parise CA, Caggiano V. Descriptive analysis of estrogen receptor (ER)-negative, progesterone receptor (PR)-negative, and HER2-negative invasive breast cancer, the so-called triple-negative phenotype: a population-based study from the California Cancer Registry. Cancer 2007;109:1721–8.
6. Dent R, Trudeau M, Pritchard KI, et al. Triple-negative breast cancer: clinical features and patterns of recurrence. Clin Cancer Res 2007; 13:4429–34.
7. Perou CM, Sorlie T, Eisen MB, et al. Molecular portraits of human breast tumours. Nature 2000;406:747–52.
8. Nautiyal J, Rishi AK, Majumdar AP. Emerging therapies in gastrointestinal cancers. World J Gastroenterol 2006;12:7440–50.
9. Slamon DJ, Leyland-Jones B, Shak S, et al. Use of chemotherapy plus a monoclonal antibody against HER2 for metastatic breast cancer that overexpresses HER2. N Engl J Med 2001;344:783–92.
10. Majumdar AP. Therapeutic potential of EGFR-related protein, a universal EGFR family antagonist. Future Oncol 2005;1:235–45.
11. Marciniak DJ, Moragoda L, Mohammad RM, et al. Epidermal growth factor receptor-related protein: a potential therapeutic agent for colorectal cancer. Gastroenterology 2003;124:1337–47.
12. Schmelz EM, Xu H, Sengupta R, et al. Regression of early and intermediate stages of colon cancer by targeting multiple members of the EGFR family with EGFR-related protein. Cancer Res 2007;67: 5389–96.
13. Xu H, Yu Y, Marciniak D, et al. Epidermal growth factor receptor (EGFR)-related protein inhibits multiple members of the EGFR family in colon and breast cancer cells. Mol Cancer Ther 2005;4:435–42.
14. Yu Y, Rishi AK, Turner JR, et al. Cloning of a novel EGFR-related peptide: a putative negative regulator of EGFR. Am J Physiol Cell Physiol 2001;280:C1083–9.
15. Zhang Y, Banerjee S, Wang Z, et al. Antitumor activity of epidermal growth factor receptor-related protein is mediated by inactivation of ErbB receptors and nuclear factor-κB in pancreatic cancer. Cancer Res 2006;66:1025–32.
16. Levi E, Mohammad R, Kodali U, et al. EGF-receptor related protein causes cell cycle arrest and induces apoptosis of colon cancer cells *in vitro* and *in vivo*. Anticancer Res 2004;24:2885–91.
17. Lombardo LJ, Lee FY, Chen P, et al. Discovery of *N*-(2-chloro-6-methyl-phenyl)-2-(6-(4-(2-hydroxyethyl)-piperazin-1-yl)-2-methylpyrimidin-4-ylamino)thiazole-5-carboxamide (BMS-354825), a dual Src/Abl kinase inhibitor with potent antitumor activity in preclinical assays. J Med Chem 2004;47:6658–61.
18. Talpaz M, Shah NP, Kantarjian H, et al. Dasatinib in imatinib-resistant Philadelphia chromosome-positive leukemias. N Engl J Med 2006; 354:2531–41.
19. Finn R, Dering J, Ginther C, et al. Dasatinib, an orally active small molecule inhibitor of both the src and abl kinases, selectively inhibits growth of basal-type/"triple-negative" breast cancer cell lines growing *in vitro*. Breast Cancer Res Treat 2007;105:319–26.
20. Huang F, Reeves K, Han X, et al. Identification of candidate molecular markers predicting sensitivity in solid tumors to dasatinib: rationale for patient selection. Cancer Res 2007;67:2226–38.
21. Johnson FM, Saigal B, Talpaz M, Donato NJ. Dasatinib (BMS-354825) tyrosine kinase inhibitor suppresses invasion and induces cell cycle arrest and apoptosis of head and neck squamous cell carcinoma and non-small cell lung cancer cells. Clin Cancer Res 2005;11:6924–32.
22. Johnson FM, Saigal B, Tran H, Donato NJ. Abrogation of signal transducer and activator of transcription 3 reactivation after Src kinase inhibition results in synergistic antitumor effects. Clin Cancer Res 2007;13:4233–44.
23. Nam S, Kim D, Cheng JQ, et al. Action of the Src family kinase

inhibitor, dasatinib (BMS-354825), on human prostate cancer cells. Cancer Res 2005;65:9185–9.
24. Shor AC, Keschman EA, Lee FY, et al. Dasatinib inhibits migration and invasion in diverse human sarcoma cell lines and induces apoptosis in bone sarcoma cells dependent on Src kinase for survival. Cancer Res 2007;67:2800–8.
25. Song L, Morris M, Bagui T, Lee FY, Jove R, Haura EB. Dasatinib (BMS-354825) selectively induces apoptosis in lung cancer cells dependent on epidermal growth factor receptor signaling for survival. Cancer Res 2006;66:5542–8.
26. Nautiyal J, Majumder P, Patel BB, Lee FY, Majumdar AP. Src inhibitor dasatinib inhibits growth of breast cancer cells by modulating EGFR signaling. Cancer Lett 2009;283:143–51.
27. Elleman TC, Domagala T, McKern NM, et al. Identification of a determinant of epidermal growth factor receptor ligand-binding specificity using a truncated, high-affinity form of the ectodomain. Biochemistry 2001;40:8930–9.
28. Majumdar APN, Banerjee S, Nautiyal J, et al. Curcumin synergizes with resveratrol to inhibit colon cancer. Nutr Cancer 2009;61:544–53.
29. Patel BB, Yu Y, Du J, Levi E, Phillip PA, Majumdar AP. Age-related increase in colorectal cancer stem cells in macroscopically normal mucosa of patients with adenomas: a risk factor for colon cancer. Biochem Biophys Res Commun 2009;378:344–7.
30. Tsao AS, He D, Saigal B, et al. Inhibition of c-Src expression and activation in malignant pleural mesothelioma tissues leads to apoptosis, cell cycle arrest, and decreased migration and invasion. Mol Cancer Ther 2007;6:1962–72.
31. Ciardiello F. Epidermal growth factor receptor inhibitors in cancer treatment. Future Oncol 2005;1:221–34.
32. Rocha-Lima CM, Soares HP, Raez LE, Singal R. EGFR targeting of solid tumors. Cancer Control 2007;14:295–304.
33. Allen LF, Lenehan PF, Eiseman IA, Elliott WL, Fry DW. Potential benefits of the irreversible pan-erbB inhibitor, CI-1033, in the treatment of breast cancer. Semin Oncol 2002;29:11–21.
34. Garrett TP, McKern NM, Lou M, et al. Crystal structure of a truncated epidermal growth factor receptor extracellular domain bound to transforming growth factor α. Cell 2002;110:763–73.
35. Biscardi JS, Tice DA, Parsons SJ. c-Src, receptor tyrosine kinases, and human cancer. Adv Cancer Res 1999;76:61–119.
36. Hennipman A, van Oirschot BA, Smits J, Rijksen G, Staal GEJ. Tyrosine kinase activity in breast cancer, benign breast disease, and normal breast tissue. Cancer Res 1989;49:516–21.
37. Messa C, Russo F, Caruso MG, Di Leo A. EGF, TGF-α, and EGF-R in human colorectal adenocarcinoma. Acta Oncol 1998;37:285–9.
38. Myoui A, Nishimura R, Williams PJ, et al. C-Src tyrosine kinase activity is associated with tumor colonization in bone and lung in an animal model of human breast cancer metastasis. Cancer Res 2003;63:5028–33.
39. Ottenhoff-Kalff AE, Rijksen G, van Beurden EACM, Hennipman A, Michels AA, Staal GEJ. Characterization of protein tyrosine kinases from human breast cancer: involvement of the c-src oncogene product. Cancer Res 1992;52:4773–8.
40. Relan NK, Saeed A, Ponduri K, Fligiel SE, Dutta S, Majumdar AP. Identification and evaluation of the role of endogenous tyrosine kinases in azoxymethane induction of proliferative processes in the colonic mucosa of rats. Biochim Biophys Acta 1995;1244:368–76.
41. Salomon DS, Brandt R, Ciardiello F, Normanno N. Epidermal growth factor-related peptides and their receptors in human malignancies. Crit Rev Oncol Hematol 1995;19:183–232.
42. Yeatman TJ. A renaissance for SRC. Nat Rev Cancer 2004;4:470–80.
43. Biscardi JS, Belsches AP, Parsons SJ. Characterization of human epidermal growth factor receptor and c-Src interactions in human breast tumor cells. Mol Carcinog 1998;21:261–72.
44. Luttrell DK, Lee A, Lansing TJ, et al. Involvement of pp60c-src with two major signaling pathways in human breast cancer. Proc Natl Acad Sci U S A 1994;91:83–7.
45. Maa MC, Leu TH, McCarley DJ, Schatzman RC, Parsons SJ. Potentiation of epidermal growth factor receptor-mediated oncogenesis by c-Src: implications for the etiology of multiple human cancers. Proc Natl Acad Sci U S A 1995;92:6981–5.
46. Muthuswamy SK, Muller WJ. Direct and specific interaction of c-Src with Neu is involved in signaling by the epidermal growth factor receptor. Oncogene 1995;11:271–9.
47. Trevino JG, Summy JM, Lesslie DP, et al. Inhibition of Src expression and activity inhibits tumor progression and metastasis of human pancreatic adenocarcinoma cells in an orthotopic nude mouse model. Am J Pathol 2006;168:962–72.